The N=28 shell closure; from N=Z to the neutron drip line

E. Caurier* and F. Nowacki†

Groupe de Physique Théorique, IReS, Bât. 27,

IN2P3-CNRS/Université Louis Pasteur,

BP 28, F–67037 Strasbourg Cedex 2, France

A. Poves‡

Departamento de Física Teórica C-XI,

Universidad Autónoma de Madrid, E–28049 Madrid, Spain

Abstract

The evolution of the N=28 neutron shell closure is studied in the N=28 isotones from neutron drip line's ^{40}Mg to N=Z doubly magic ^{56}Ni. It is found that the N=28 closure vanishes at Z=12 in favor of a deformed ground state. For Z=14 and Z=16 closed shell and intruder configurations are almost degenerate, leading to highly mixed ground states and to very low lying excited 0^+ states. For Z>20 the intruder states are always above the closed shell ground states. We examine their structure and their possible existence as collective yrare bands of well defined particle-hole character.

PACS numbers: 21.10.–k, 27.40.+z, 21.60.Cs, 23.40.–s

*Electronic address: `etienne.caurier@ires.in2p3.fr`

†Electronic address: `frederic.nowacki@ires.in2p3.fr`

‡Electronic address: `alfredo.poves@uam.es`

I. INTRODUCTION

The fate of the magic closures far from stability is an issue of great current experimental and theoretical activity. Harmonic oscillator shell closures have been shown not to hold in the neutron rich regions (^{11}Li and ^{12}Be at N=8; ^{31}Na and ^{32}Mg at N=20; ^{68}Ni at N=40) as well as in the proton rich side (^{80}Zr at N=Z=40). Spin-orbit closures (28, 50 82, 126) seemed until now to be more robust. How can a shell closure disappear? It depends on the balance of two opposite tendencies. On one side magic numbers are associated to energy gaps in the spherical mean field, this means that to promote particles above a closed shell, costs energy. However, this energy can be partly recovered, because closed shells have no correlation energy, while open shell configurations of neutrons and protons have a lot. For instance, in ^{80}Zr, the gap between the pf-shell and the $1g_{9/2}$ orbit is greatly reduced as a consequence of the very attractive spin-orbit interaction. This makes it energetically favourable to promote particles beyond the pf-shell to take advantage of the large quadrupole and pairing correlations. Indeed, ^{80}Zr is found experimentally to be a well deformed rotor, consistent with a large occupancy of the $1g_{9/2}$ orbit and its quadrupole partners.

At the neutron rich edge, the structure of the spherical mean field may be at variance with the usual one at the stability line. The reason is that at the stability line the T=0 channel of the nucleon-nucleon interaction has a stronger weight relative to the T=1 channel than it has when the neutron excess is very large. When some of the gaps get reduced, open shell configurations, usually two neutron excitations across the neutron closure, take advantage of the availability of open shell protons to build highly correlated states that are more bound than the closed shell configuration. Then the shell closure is said to have vanished. ^{31}Na is a reference case for this physics.

In this article we shall address the question of the persistence of the N=28 shell closure. It is the first spin-orbit driven "classical" closure. In combination with the N=20 harmonic oscillator closure it produces the doubly magic ^{48}Ca, while at N=Z leads to ^{56}Ni. ^{68}Ni, another potential doubly magic nuclei does not appear to be one, while ^{78}Ni is believed to be doubly magic again. In addition we shall examine the structure of the states that can compete with, and even beat the magic closure, whether they correspond to intrinsic structures or not and whether they keep their identity in the spectra even if they do not become ground states.

TABLE I: N=28 isotones: quasiparticle neutron gaps, difference in correlation energies between the 2p-2h and the 0p-0h configurations and their relative position

	^{40}Mg	^{42}Si	^{44}S	^{46}Ar	^{48}Ca	^{50}Ti	^{52}Cr	^{54}Fe	^{56}Ni
gap	3.35	3.50	3.23	3.84	4.73	5.33	5.92	6.40	7.12
ΔE_{Corr}	8.45	6.0	6.66	5.98	4.08	7.59	10.34	10.41	6.19
E^*_{2p-2h}	-1.75	1.0	-0.2	1.7	5.38	3.07	1.50	2.39	8.05

II. THE N=28 ISOTONES

Our starting point is ^{48}Ca, one of the strongest closures in the nuclear chart. To the proton rich side we can reach ^{56}Ni, while to the neutron rich side we could aim to doubly magic ^{36}O, were it not because this nucleus is well beyond the neutron drip line, as it is also the case of ^{38}Ne. For Z$\leq$20 we use a valence space comprising the pf-shell for the neutrons and the sd-shell for the protons. The interaction is described in [1]. For Z>20 we use the pf-shell for neutrons and protons and the interaction KB3G [2]. The intruder configurations are characterised by imposing that two neutrons be *outside* the $1f_{7/2}$ neutron orbit.

The diagonalizations are performed in the m-scheme using a fast implementation of the Lanczos algorithm through the code ANTOINE [3, 4] or in J-coupled scheme using the code NATHAN [4]. Some details may be found in ref. [5]. The Lanczos Strength Function (LSF) method, following Whitehead's prescription [6], is explained and illustrated in refs. [7–9].

We shall examine first the results gathered in Table I. In our reference magic nucleus, ^{48}Ca, the intruder configuration is 5.38 MeV less bound than the closed shell. This number results of subtracting two contributions: Promoting two particles across the N=28 neutron closure, represents an energy loss of twice the value of the gap (4.73 MeV in our calculation). On the other side, the intruder configuration gains 4.08 MeV of correlation energy (mainly due to pairing) relative to the closed shell. When full mixing is allowed, the ground state of ^{48}Ca remains a closed shell at 90%.

Adding protons to ^{48}Ca increases the neutron gap. The correlation energy of the intruder state grows also rapidly to reach 10.32 MeV in ^{52}Cr, it remains almost constant in ^{54}Fe and drops abruptly at the proton closure in ^{56}Ni. In all the cases the intruder configuration is less bound than the closed shell. It is at mid-proton shell where the energy difference is smaller (1.5 MeV). After mixing, the first excited 0^+ state of ^{52}Cr, dominated by the intruder configurations, lies at 2.43 MeV, compared to the experimental value 2.65 MeV. Similar degree of accord with experiment is found in ^{54}Fe (2.80 MeV *vs* 2.56 MeV) and ^{50}Ti (4.08 MeV *vs* 3.87 MeV). The case of ^{56}Ni is different because the first excited 0^+ state is predominantly 4p-4h. Its correlation energy is very large. Depending on the effective interaction used, the fully mixed results give a 60-70% of doubly magic closure its ground state.

When protons are removed from ^{48}Ca, then N=28 neutron gap first diminishes and then remains constant at about 3.5 MeV. The correlation energy of the intruder increases in ^{46}Ar and ^{44}S and then goes down slightly at the proton sub-shell closure in ^{42}Si. Finally it rises abruptly at ^{40}Mg. The resulting scenarios are quite diverse. In ^{46}Ar the intruder is clearly above the closed shell, in ^{44}S they are almost degenerate, in ^{42}Si the closed shell takes over again by little and in ^{40}Mg the intruder state is well below the closed shell.

III. THE STRUCTURE OF THE INTRUDER STATES

The states that challenge the shell closure have large correlation energy. Large correlation energy is most often related to large quadrupole coherence. If this were the case here, the vanishing of the N=28 shell closure would be accompanied of a transition from spherical to deformed shapes or would result in a strong case of coexistence.

In order to understand this issue we first calculate the spin sequences 0^+, 2^+, 4^+, etc. in the basis of all the configurations that have two neutrons outside the $1f_{7/2}$ orbit. Our conclusions about the collective character of the bands will be based on the analysis of the excitation energies, the static quadrupole moments and the E2 transition probabilities, that we have gathered in Table II for Z>20 and in Table III for Z<20.

In ^{54}Fe we face a clear-cut example of rotational structure that stands up to spin J=8. The static and dynamic (transition) quadrupole moments, which can be extracted from the spectroscopic quadrupole moments and B(E2)'s using the standard formulae (see ref. [10]), are nicely constant and correspond roughly to a deformation β=0.3. We can therefore conclude that the lowest intruder band in ^{54}Fe has a prolate intrinsic structure. How it manifests in the physical spectrum will be the topic of the next section. Similar conclusions hold when we move to ^{52}Cr, whose intruder state is an even better rotor and slightly more deformed. On the contrary, the intruder band in ^{50}Ti is less convincing. It has some rotational flavor, but not enough to conclude that it represent a “bona fide” intrinsic state.

TABLE II: Properties of the intruder states of 2p-2h character in ^{54}Fe, ^{52}Cr and ^{50}Ti. Excitation energies in MeV, B(E2)'s in $e^2\, fm^4$, Spectroscopic quadrupole moments in $e\, fm^2$.

	^{54}Fe			^{52}Cr			^{50}Ti		
J	ΔE	Q	B(E2)↓	ΔE	Q	B(E2)↓	ΔE	Q	B(E2)↓
0	0.00			0.00			0.00		
2	0.51	-30.0	224	0.40	-30.7	235	0.53	-20.6	128
4	1.51	-36.9	312	1.19	-38.5	331	1.39	-23.8	188
6	2.85	-38.3	321	2.33	-40.0	339	2.36	-22.6	185
8	4.48	-35.0	294	3.81	-37.3	319	3.51	-26.6	161

TABLE III: Properties of the intruder states of 2p-2h character in ^{46}Ar, ^{44}S, ^{42}Si and ^{40}Mg. Excitation energies in MeV, B(E2)'s in $e^2\, fm^4$, Spectroscopic quadrupole moments in $e\, fm^2$.

	^{46}Ar			^{44}S			^{42}Si			^{40}Mg		
J	ΔE	Q	B(E2)↓	ΔE	Q	B(E2)↓	ΔE	Q	B(E2)↓	ΔE	Q	B(E2)↓
0	0.00			0.00			0.00			0.00		
2	0.81	-8.70	61	0.73	-19.0	97	0.96	-9.44	38	0.65	-19.3	95
4	2.00	0.82	80	2.13	-21.5	129	2.13	-4.60	38	1.92	-22.2	125
6	2.75	22.5	41	4.16	-10.0	100	2.62	18.3	15	3.44	-0.89	78
8	4.45	21.2	81	6.73	-7.74	64	4.70	9.18	21	5.01	-4.48	74

The situation becomes more involved in the Z<20 isotones, because of the influence of the filling of the proton orbits on the structure of the intruders. In ^{46}Ar and ^{42}Si there is no signal of any intrinsic state. On the contrary, in ^{44}S and ^{40}Mg the sequence 0^+, 2^+, 4^+ exhibits clear rotational features corresponding to β=0.35. The rotational behaviour of the bands is somehow blurred at J=6-8. Indeed, for the lower spins we are entitled to speak of deformed intruder bands.

What happens to these bands (or states) when full mixing is allowed? Or, in other words, what is the structure of the physical spectra according to our calculations? This aspect is better explained by figures 1 and 2, where we have plotted the projection of the the lowest closed shell 0^+ state (upper panel) and the lowest intruder 0^+ state (bottom panel) onto the physical 0^+ states. The projections are obtained by means of the Lanczos strength function method. The spikes give the squared overlap of these two states with the physical states. In figure 1 we present the results for ^{50}Ti ^{52}Cr and ^{54}Fe and in figure 2 for ^{46}Ar, ^{44}S, ^{42}Si, and ^{40}Mg.

The results for all the isotopes with Z>20 are quite similar; The closed shell configuration is dominant in the ground state (about 70%), nothing unexpected. What may be a bit more surprising is that the intruder 0^+ state dominates the first excited 0^+ state, even more strongly (about 75%). The same happens for the other spin values. The lowest physical state of each spin is dominated by the closed shell configuration while the intruder state has large overlap with a single physical state. This may indicate that these intruder structures can survive to the mixing with the huge number of configurations in the model space, keeping their identity as collective yrare bands, and providing a good example of coexistence of spherical and deformed shapes.

In Figure 2, ^{46}Ar shows already a larger degree of mixing between the closed shell and the 2p-2h bandhead, nonetheless, the former is still dominant in the physical ground state. The 2p-2h 0^+, is split between the 0^+_2 and 0^+_3 physical states. The ground state of ^{44}S is an even mixture of the (spherical) closed shell 0^+, and the deformed 2p-2h 0^+ bandhead. The low lying 0^+_2 has the same amount of mixing. This is a rather unusual situation provoked by the near degeneracy of the two states before mixing. A similar situation occurs in ^{42}Si, except that now the 2p-2h 0^+ does not correspond to a deformed shape. On the contrary, the ground state of ^{40}Mg is fully dominated by the deformed 2p-2h 0^+ bandhead. This dominance is maintained up to J=6. Hence a very simple picture emerges; the deformed intruder band that was yrare near the stability becomes yrast at the neutron drip line; the shape transition has finally happened. This kind of inversion of spherical and deformed configurations, leading to shape transitions, takes also place in the other neutron rich semi-magic Magnesium isotope ^{32}Mg (N=20).

Another striking prediction of our calculations is the occurence of a superdeformed band in ^{42}Si of 4p-4h nature. Contrary to the 2p-2h structure analysed above, that wasn't deformed

TABLE IV: N=28 isotones: Calculated spectra, quadrupole properties and occupancies of the Z<20, N=28, isotones.

	^{40}Mg	^{42}Si	^{44}S	^{46}Ar
$E^*(2^+)$(MeV)	0.81	1.49	1.22	1.51
$E^*(4^+)$	2.17	2.68	2.25	3.46
$E^*(0^+_2)$	1.83	1.57	1.26	2.93
$Q(2^+)$(e fm^2)	-21	16	-17	20
B(E2)(e^2 fm^4)	108	71	93	93
$\langle n_{7/2}\rangle$	5.54	6.16	6.16	6.91
$(f_{7/2})^8$ %	3	28	24	45

due to the $1d_{5/2}$ proton orbit closure, the 4p4h configuration has open shell protons and neutrons and attains a large deformation. In addition, when mixing in the full space is allowed, the band stands with even enhanced deformation. The rotational bandhead is located at an excitation energy of 5 MeV. The band is caracterized by an intrinsic quadrupole moment Q_0 of 86 $e\ fm^2$ (corresponding to a deformation parameter $\beta \sim 0.5$) and terminates at spin $8\hbar$.

Finally, we gather in Table IV some numerical results for the Z<20 isotones. Notice in particular the near degeneracy of the first excited 2^+ and 0^+ states in ^{44}S and ^{42}Si and the complete disappearance of the closed shell component in the ground state of ^{40}Mg already apparent in Figure 2.

IV. COLLECTIVE YRARE BANDS IN ^{52}CR AND ^{54}FE

The occurrence of yrare bands of enhanced collectivity, with a well defined particle-hole structure on top of the ground state, has been recently documented by experiments in ^{56}Ni [11], ^{36}Ar [12] and ^{40}Ca [13]. In the Nickel and Argon cases the bands are dominantly made of 4p-4h excitations while in ^{40}Ca the leading structure is 8p-8h [14]. In ^{56}Ni the band is classified as highly deformed β= 0.3/0.4 , while in ^{36}Ar and ^{40}Ca they are characterised as superdeformed with β= 0.4/0.5 and β= 0.5/0.6 respectively. In a recent study [15], Mizusaki and co-workers have carried out a theoretical search for this kind of bands in the

N=28 isotopes, using the Monte Carlo shell model approach. According to their calculations with the FPD6 interaction [16] the 2p-2h collective bands of ^{52}Cr and ^{54}Fe, that we have studied in the preceding section persist in the full calculation (actually it is not very clear in their paper if the results are from MCSM calculations or from direct diagonalizations, that should involve truncations at least in ^{54}Fe). They discuss also the possible existence of another yrare band in ^{54}Fe, this time of 4p-4h nature. Their conclusion is positive, but based only on a mean field calculation with incorporates variation after projection (VAP) because (sic) the MCSM is impractical in this case. We will reexamine this problem as a natural continuation of our present study.

The calculation of yrare bands in nuclei with large shell model dimensionalities, poses serious computational problems. The reason is that, most often, the interesting states lie at excitation energies where the level density is high. This represents a real challenge for all the shell model approaches, because it requires the calculation of many states of the same spin and parity. While this can be easily done for m-scheme dimensions of a few tens of millions, the task becomes formidable for dimensions of hundreds of millions. The method of ref [15] relies in the existence of local minima in the projected energy surfaces resulting of a constrained Hartree-Fock calculation. The Slater determinants corresponding to these minima are then fed into the MCSM.

In our approach, we first compute as many fully converged 0^+ states as necessary to obtain the band-heads of the potential yrare bands. To select them, we apply the quadrupole operator and use the LSF method to decide if there is a dominant branch connecting them to a 2^+ state that would then be a member of the band. We proceed upwards in spin until the collective transition strength diminish drastically or bifurcates. In the case of the 2p-2h bands we have already shown that the band-heads are the first excited 0^+'s.

In ^{52}Cr the calculations are carried out in the full pf-shell (m-scheme dimension 45 millions). The 2p-2h band-head at 2.43 MeV, is in correspondence with the experimental 0^+_2 at 2.65 MeV. It has a 46% content of 2p-2h, 26% of 3p-3h, 18% of 4p-4h and minor percentages of the other components. Besides the "coherent" 2p-2h state, the next four 0^+ states produced by the calculation are also in correspondence with the experimental 0^+'s:

0^+_3; exp. 4.74 MeV; th. 5.15 MeV,

0^+_4; exp. 5.60 MeV; th. 5.47 MeV,

0^+_5; exp. 5.75 MeV; th. 6.04 MeV,

$$0_6^+;\ \text{exp. } 6.10\ \text{MeV};\ \text{th. } 6.30\ \text{MeV},$$

providing a rather spectacular showpiece of shell model spectroscopy.

Let's see how the procedure works. First we apply the quadrupole operator to the 0^+ bandhead: $Q|0^+\rangle$. This operation generates a threshold vector that we take as the "pivot" in the Lanczos procedure. We perform N$\sim$100 iterations to produce an approximate strength function. At this stage, either there is one state that carries most of the strength, thus belonging to the band, or not, in which case there is no band. In the positive case the resulting $|2^+\rangle$ state is retained as a band member and we proceed to act with Q on it. In this step, there are several possible angular momentum couplings, and we follow the ΔJ=2 path in the even-even nuclei. The procedure is repeated until the strength bifurcates, dilutes or plainly disappears.

In ^{52}Cr we can definitely speak of a "theoretical" yrare band. Our results for the excitation energies are very close to those of ref. [15]. In table V we list the excitation energies, the percentage of the B(E2)$\uparrow$ of the transition from J-2 to J carried by each state, the amount of 2p-2h components, the B(E2)$\downarrow$ and the spectroscopic quadrupole moments. All these numbers are consistent with a deformed band up to J=10, afterwards a bifurcation and reduction of the strength takes place. Notice the large B(E2) values, similar to those of the

TABLE V: Yrare 2p-2h band in ^{52}Cr. Excitation energies are relative to the 0_2^+ band-head, experimentally at 2.64 MeV and calculated at 2.43 MeV. Energies in MeV, B(E2)'s in $e^2\,fm^4$, Q's in $e\,fm^2$

J	ΔE	% of B(E2)$\uparrow$	% of 2p-2h	B(E2)$\downarrow$	Q_{spec}
0	0.00		46		
2	0.44	77	43	238	-27.7
4	1.32	82	43	323	-39.3
6	2.51	77	42	329	-39.3
8	4.14	83	44	331	-39.2
10	6.03	66	39	239	-25.5
12	8.02	27	51	66	-13.7
12	8.31	28		69	

yrast band of ^{48}Cr, corresponding to $\beta \sim 0.3$. Besides, the energy spacings are very close to those of a rigid rotor;

$$\frac{\Delta E(4^+)}{\Delta E(2^+)}{=}3(3.33);$$
$$\frac{\Delta E(6^+)}{\Delta E(4^+)}{=}1.9(2.1);$$
$$\frac{\Delta E(8^+)}{\Delta E(6^+)}{=}1.65(1.71);$$
$$\frac{\Delta E(10^+)}{\Delta E(8^+)}{=}1.46(1.53);$$

(the values in parenthesis are those of the rigid rotor limit). The percentage of the 2p-2h components as well as the occupation numbers of the individual orbits are nicely constant too. The spectroscopic quadrupole moments correspond to a prolate rotor and are fully consistent with the B(E2)'s. The sequence of calculated states, 0^+ at 2.43 MeV, 2^+ at 2.87 MeV, 4^+ at 3.75 MeV and 6^+ at 4.94 MeV can be put in correspondence with the experimental ones at 2.64 MeV (0^+), 3.16 MeV (2^+), 4.04 MeV (4^+) and 5.14 MeV (6^+). However, there are no transitions experimentally observed linking these states. This means that, due to the presence of many other 2p-2h states to which to decay by M1 transitions and to the phase space enhancement of the E2 transitions to the yrast band, the "theoretical" yrare band does not show up experimentally as a γ-cascade.

We have also searched for other bands of 4p-4h nature but we have found none compatible with our requirements.

For ^{54}Fe the full space calculations of the different strength functions demand a computational effort beyond our present means. However, we have verified in ^{52}Cr and in other cases that it is accurate enough to compute them at the truncation level t=n+4 (t is the number of particles that can be excited from the $1f_{7/2}$ orbit to the rest of the pf-shell and n is the np-nh character of the band). Hence, we can use t=6 for the 2p-2h and t=8 for the 4p-4h cases (m-scheme dimension 177 millions). The situation for the lowest yrare band resembles that of ^{52}Cr; the coherent 2p-2h state represents 43% of the 0^+_2 at 2.77 MeV (exp. at 2.56 MeV). The yrast band is also well reproduced by the calculation with the KB3G interaction; the states 2^+ at 1.52 MeV, 4^+ at 2.26 MeV and 6^+ at 3.02 MeV agree nicely with the experimental ones at 1.41 MeV (2^+), 2.54 MeV (4^+) and 2.95 MeV (6^+). The results for the yrare band are gathered in Table VI. The 2^+-0^+ splitting of 0.55 MeV can be

TABLE VI: Yrare 2p-2h band in ^{54}Fe. Excitation energies are relative to the 0^+_2 band-head, experimentally at 2.56 MeV and calculated at 2.77 MeV. Energies in MeV, B(E2)'s in $e^2\,fm^4$, Q's in $e\,fm^2$

J	ΔE	% of 2p-2h	B(E2)↓	Q_{spec}
0	0.00	45		
2	0.55	43	232	-29.1
4	1.57	37	262	-29.9
6	3.07	40	298	-40.5
8	4.00	35	205	-22.4

put in correspondence with the experimental 2^+_3-0^+_2 splitting (0.61 MeV). As in the case of ^{52}Cr, there is no doubt about the collective character of this "theoretical" yrare band, even is some rotational features are less perfect than in ^{52}Cr, for instance, the band is completely disolved beyond J=8. No in-band transitions are experimentally seen, for the same reasons advocated for ^{52}Cr.

We have made a very thorough search for more deformed yrare bands of 4p-4h character also in ^{54}Fe, motivated by the prediction made in ref [15] using the FPD6 interaction and a deformed Hartree-Fock calculation with variation after projection to good angular momentum (VAP). Indeed, if we do a calculation with the same interaction and a fixed number of particles outside the $1f_{7/2}$ orbit equal to four, we find a collective band with a B(E2)($2^+ \rightarrow 0^+$)≈ 400 e^2 fm^4 which is not far from the VAP result ≈ 500 e^2 fm^4. However, when we perform a –nearly- full calculation (t=8), fully converging all the 0^+ and 2^+ states up to 7 MeV of excitation energy (eight 0^+'s and fifteen 2^+'s) the 4p-4h band members are completely fragmented among the physical states and no trace of any other collective structure is found in the results. With the only caveat of the non-completeness of the calculation in the pf-shell, we can refute the VAP prediction, that, obviously, is far from including the mixing present in the shell model calculations.

In summary, we have studied the occurrence of collective yrare bands of well defined p-h character in the N=28 isotones. We have confirmed the existence of deformed 2p-2h yrare bands in ^{52}Cr and ^{54}Fe. However they don't show up experimentally as such; the states decay preferentially out of the band due to the phase space enhancement. In ^{40}Mg the 2p-2h band actually becomes yrast, producing a spherical to deformed shape transition at the drip line, while the N=28 closure vanishes.

Acknowledgements. This work has been partly supported by MCyT (Spain), grant BFM2000-30 and by the IN2P3 (France)-CICyT (Spain) agreements. We also thank the CCC-UAM for a computational grant.

---

[1] S. Nummela et al., Phys. Rev. C **63** (2001) 044316.

[2] A. Poves, J. Sánchez Solano, E. Caurier and F. Nowacki, Nucl. Phys. A **694** 157 (2001) 157.

[3] E. Caurier, shell model code ANTOINE, IRES, Strabourg 1989-2002

[4] E. Caurier and F. Nowacki, Acta Physica Polonica B, Vol. 30, 3 (1999) 705.

[5] E. Caurier, G. Martínez-Pinedo, F. Nowacki, A. Poves, J. Retamosa and A. P. Zuker, Phys. Rev. C **59** (1999) 2033.

[6] R.R. Whitehead, *Moment methods in many fermion systems*, B. J. Dalton et al. eds. (Plenum, New York, 1980).

[7] E. Caurier, A. Poves and A. P. Zuker, Phys. Lett. B **256** (1991) 301.

[8] E. Caurier, A. Poves and A. P. Zuker, Phys. Lett. B **252** (1990) 13.

[9] S.D. Bloom and G.M. Fuller, Nucl. Phys. A **440** (1985) 511.

[10] A. Bohr and B. Mottelson, *Nuclear Structure* Vol. II (Benjamin, New York, 1975).

[11] D. Rudolph *et al.*, Phys. Rev. Lett. **82** (1999) 3763.

[12] C. E. Svensson *et al.*, Phys. Rev. Lett. **85** (2000) 2693.

[13] E. Ideguchi *et al.*, Phys. Rev. Lett. **87** (2001) 222501.

[14] E. Caurier, F. Nowacki, A. Poves and A. Zuker, The superdeformed excited band of Ca-40, nucl-th 0205036.

[15] T. Mizusaki, T. Otsuka, M. Honma and B. A. Brown, Phys. Rev. C **63** (2001) 044306.

[16] W. A. Richter, M. G. van der Merwe, R. E. Julies, and B. A. Brown, Nucl. Phys. A **523** (1991) 325.

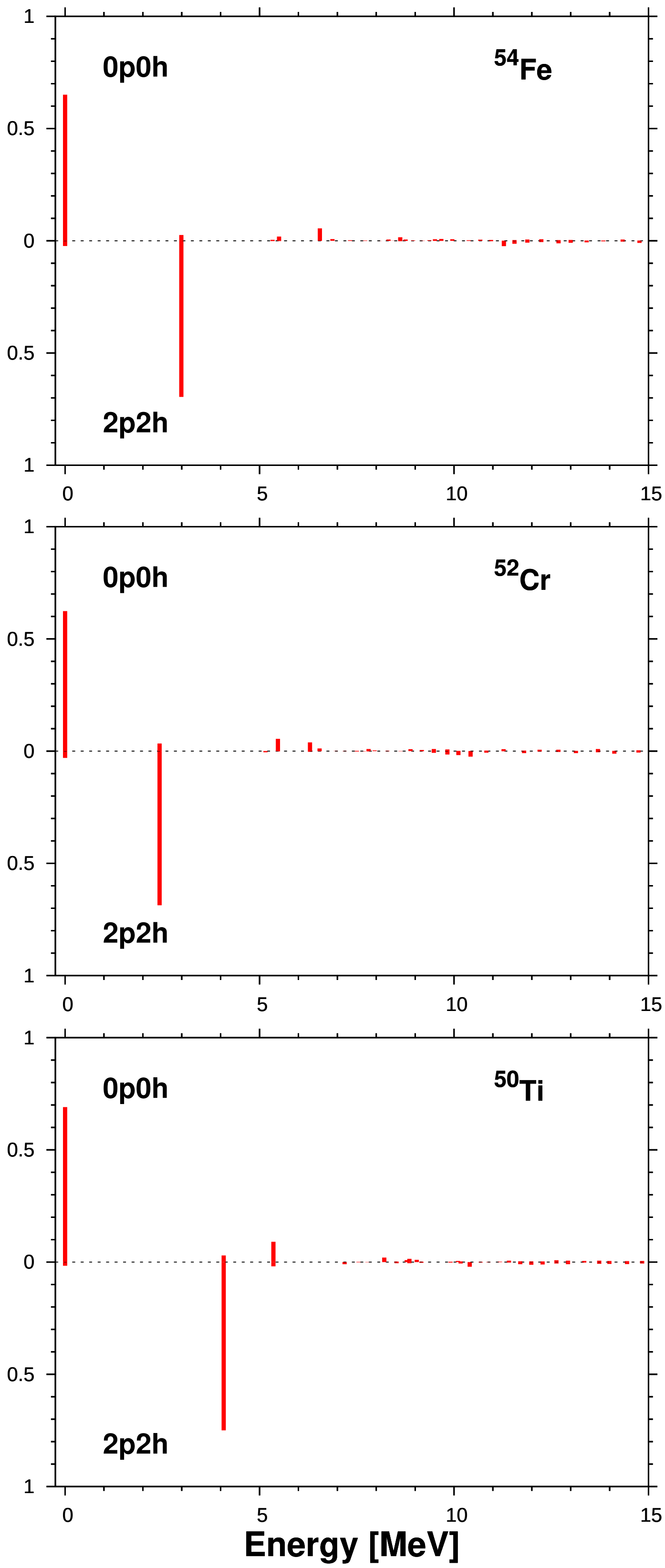

FIG. 1: Overlaps (squared) of the closed shell 0^+ (upper panels) and the intruder 0^+ (bottom panels) with the physical 0^+ states in ^{50}Ti, ^{52}Cr and ^{54}Fe

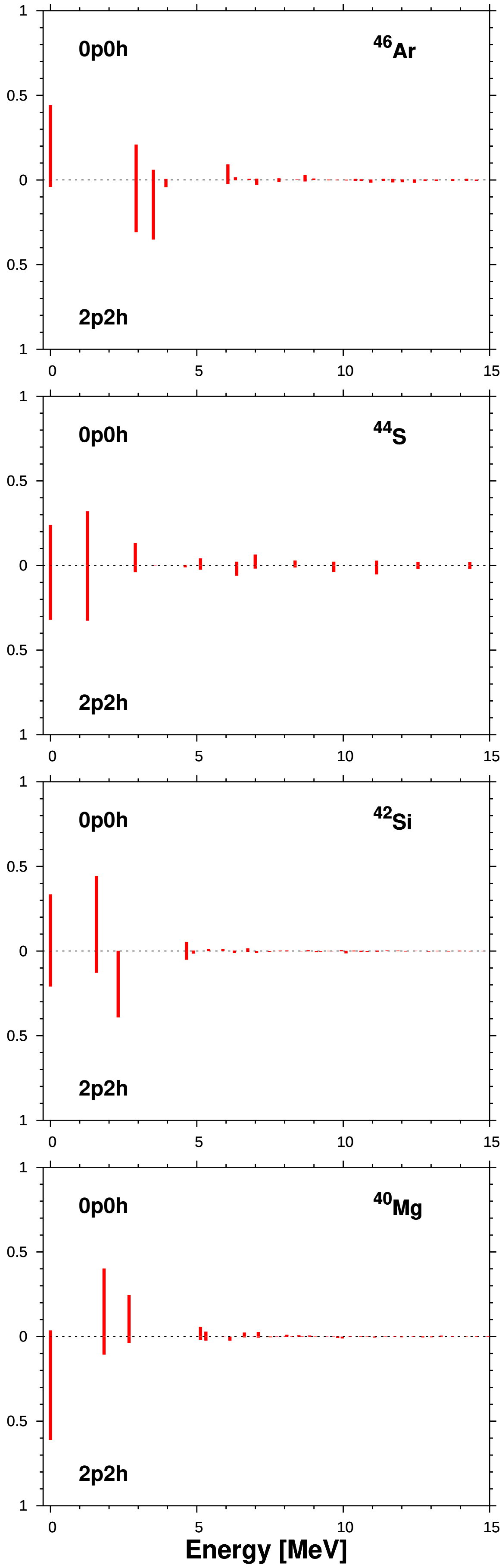

FIG. 2: Overlaps (squared) of the closed shell 0^+ (upper panels) and the intruder 0^+ (bottom panels) with the physical 0^+ states in ^{46}Ar, ^{44}S, ^{42}Si, and ^{40}Mg